The Impacts of Chase Combining-based Retransmissions on LoRaWAN Performance

Elvis M. G. Stancanelli, Francisco Helder C. dos S. Filho

[1]Federal University of Ceará (UFC) – Campus Quixadá
63902-580 – Quixadá – Brazil

`{elvis.stancanelli,helderhdw}@ufc.br`

Abstract. *LoRaWAN technology stands out in wireless communication applications due to its low power consumption and long-range capabilities. However, using a retransmission mechanism to ensure reliable communication can increase overhead and computational complexity, negatively impacting throughput and energy efficiency. Achieving a balance between reliability and scalability poses a challenge in LoRaWAN. One probable solution to this challenge is implementing a soft combination of retransmitted versions, prioritizing reliability characteristics. However, this approach has not yet been explored in LoRaWAN. This study examines the potential impacts of utilizing a popular soft combination of retransmission in LoRaWAN, called chase combining, and assesses its reliability and efficiency. The numerical analysis indicates that the spread factor significantly affects the advantages of chase combining. The study's outcomes suggest that appropriately using chase combining can significantly improve the success rates of packets. However, this may lead to a minor trade-off regarding increased latency and energy consumption.*

1. Introduction

Low Power Wide Area Network (LPWAN) technology initially surfaced as a compliment to traditional cellular and short-range wireless technologies, designed to cater to the diverse requirements of Internet of Things (IoT) applications [de Castro Tomé et al. 2018]. Presently, LPWAN has gained a significant foothold in wireless communication applications in which slight power consumption is prioritized over high data rates or extremely low latencies.

LoRaWAN (Long Range Wide Area Network)[Alliance 2018b] is a leading technology in LPWANs, operating on unlicensed Industrial, Scientific, and Medical (ISM) frequency bands and offering long-range communication with low power consumption. When dealing with service traffic, it is important to closely observe the reliability and efficiency of LoRaWAN, as they are two critical aspects. Different packets prioritize varying proportions of these aspects, putting emphasis on the transmission rates and the assurance that the package will be received. Our primary focus is on the uplink, representing a crucial sensing component. Therefore, the retransmission mechanism can be a strong ally in reliably receiving alarm messages.

Hybrid Automatic Repeat reQuest (HARQ) is a mechanism that joints forward error correction and automatic repeat requests, allowing a balance between these critical aspects. In essence, HARQ is a communication protocol permitting the retransmission of

lost or corrupted frames or packets, which should play a central role in addressing challenges associated with channel impairments and packet loss in LoRaWAN networks. The HARQ mechanism provides a robust means to overcome environmental interferences and fast fading, ensuring reliable data transmission. HARQ can be a potent ally in ensuring the receipt of critical messages. As the IoT evolves, HARQ becomes increasingly significant, laying the groundwork for a connected and intelligent future.

Although HARQ is not yet incorporated into LoRaWAN, LoRa Alliances specifies the acknowledgment procedure [Alliance 2018a] ordered by the network server or an application server: "When receiving a confirmed data message, the receiver shall respond with a data frame that has the acknowledgment bit (ACK) set." That specification does not mention any Negative ACK signal, which forces one to wait a pre-established period before starting a new transmission. In order to confirm an uplink frame, ACK must be sent to the end-device using one of the receive windows opened after the send operation. The end-device performs frequency hopping between repeated transmissions and waits until the receive windows expire.

Ahmed et al. [Ahmed et al. 2021] surveyed the research works exploring HARQ for a broad scope of applications in wireless communications, briefly including emerging technologies such as ultra-reliable, low-latency, cooperative, and massive machine-type communications. The authors discuss the advantages and disadvantages of HARQ and address the open problems and future research directions. However, issues inherent to LoRa, such as quasi-orthogonality, time-on-air, and segregation by SF, have not been addressed therein. In [Paul 2020], Paul provided a mathematical model to predict the impacts of packet retransmissions on packet collision rate in LoRaWAN. [Capuzzo et al. 2018] simulated the performance of a LoRaWAN, showing its degradation when the confirmed traffic increases. This behavior suggests a more rational use of confirmed traffic, and the maximum number of transmission attempts becomes a critical parameter. In order to reduce the overhead due to many ACKs, aggregating ACKs in a simple acknowledgment containing multiple device addresses is more interesting than sending multiple ACKs, as investigated in [Abdelfadeel et al. 2020, Lee et al. 2021].

The potential of a soft combination of diverse received versions of a message in LoRaWAN has been missed by academia, leading to discarded valuable information. Whether it is waiting for reinforcement or not, even these rejected packets can contain helpful information, which may not be valid on its own but can be combined with other pieces of information to create a more reliable and accurate result. Incorporating Hybrid Automatic Repeat Request (HARQ) allows for a soft combination of all sent versions, thus enhancing the performance potential. This approach emphasizes the importance of not overlooking any data, as every piece of information can improve network performance, no matter how seemingly insignificant.

This paper delves into the research path towards incorporating HARQ into LoRa. As LoRa is a proprietary solution that does not allow fundamental changes, we used a LoRaWAN computational simulation tool to model the HARQ mechanism and evaluate its potential impacts. We simulated the chase combining retransmission technology with all required feedback channels and signaling under a maximum of three retransmissions. We measured the changes in packet loss and data rate, as well as we estimated the impacts on energy consumption. The numerical results confirmed that implementing HARQ re-

transmission in LoRaWAN is beneficial in terms of reliability, efficiency, and scalability.

The remaining part of this paper is structured as follows: Section 2 introduces the technical details of LoRa and LoRaWAN. Section 3 presents the system model used here. Section 4 presents our numerical results and discusses the benefits and drawbacks of retransmission on LoRaWAN. Section 5 concludes this paper.

2. Overview about LoRaWAN

As mentioned in the LoRa Alliance [Alliance 2018b] website[1]: "The LoRaWAN® specification is a Low Power, Wide Area (LPWA) networking protocol designed to wirelessly connect battery operated 'things' to the internet in regional, national or global networks, and targets key Internet of Things (IoT) requirements such as bi-directional communication, end-to-end security, mobility and localization services."

The LoRaWAN network architecture follows a star-of-stars topology (see Figure 1), whose gateways relay messages between end-devices and a central network server. Gateways and network servers are connected, operating standard IP connectivity. The gateways are in charge of converting radio-frequency packets to IP packets and vice-versa. Conversely, end-devices are connected to one or many gateways [Alliance 2018a].

Among many other features, LoRaWAN specifies medium access control (MAC) and message formats delivered through a proprietary physical layer called LoRa. Semtech Corporation is responsible for LoRa[2], whereas LoRa Alliance continually updates LoRaWAN specifications [Alliance 2018b].

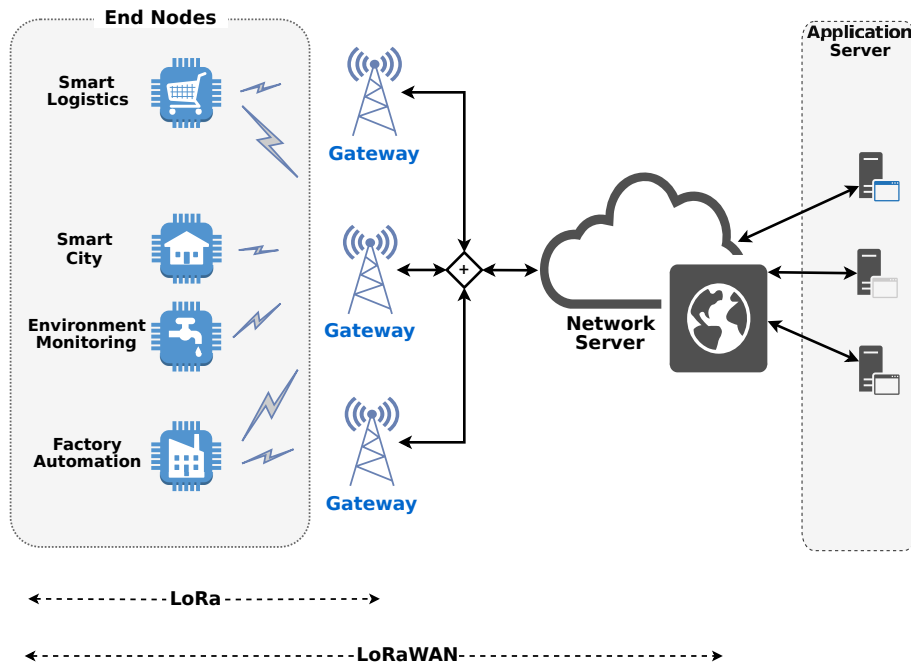[1]https://lora-alliance.org/about-lorawan/
[2]https://www.semtech.com/lora

Figure 1. LoRaWAN architecture with the main elements: end-nodes illustrated by sensors, gateways (depicted as base stations), network server (NS).

2.1. LoRa

LoRa is a proprietary physical layer derived from Chirp Spread Spectrum, one variant of spread spectrum technology, making the whole system robust to interference and thermal noise. The message from each device is encoded by a linearly increasing frequency modulated chirp pulse, the up-chirp, whereas a down-chirp is reserved for further decoding. Spreading factor (SF) is the ratio of the bandwidth to the data rate, used as an integer ranging from 7 to 12.

Once it is spread in the spectrum, the LoRa signal occupies the entire frequency band designated for it; some of the bandwidths adopted are [Adelantado et al. 2017]: 125 kHz, 250 kHz, and 500 kHz. At the end of the transmission chain, the LoRa signal respective to the binary message $w(nT_s)$ and given SF is expressed by [Vangelista 2017]:

$$c(nT_s + kT) = \frac{1}{\sqrt{2^{SF}}} \exp\left\{ j2\pi \left[\left(k + \sum_{h=0}^{SF-1} w(nT_s)_h \cdot 2^h \right) \mod 2^{SF} \right] \frac{k}{2^{SF}} \right\}, \quad (1)$$

in which k ranges from 0 to $2^{SF} - 1$, $w()_h$ denotes h^{th} bit of the binary message and A mod B refers to the remainder of the division A/B.

LoRa receiver checks the similarity of the received signal with all down-chirp pulses through the correlation operation with each of them. Transmissions with different spreading factors are said to be quasi-orthogonal to each other, improving the network capacity. Besides the quasi-orthogonality, sensitivity is another key factor of LoRa link [Mahmood et al. 2018][Croce et al. 2018]. The sensitivity thresholds can be obtained from Semtech's datasheet [Semtech 2017], as gathered in Table 1.

The nominal bit rate of LoRa ranges from 0.3 kbps to 27 kbps. For a modulation bandwidth (BW), the rates R_b is a function of the spreading factor (SF) employed, and is given by [Haxhibeqiri et al. 2018]:

$$R_b = \text{SF} \cdot \left(\frac{4}{4 + \text{CR}_i} \right) \cdot \left(\frac{\text{BW}}{2^{\text{SF}}} \right), \quad (2)$$

in which CR_i is the code rate index that can take integer values from 1 to 4.

For a given combination of spreading factor, coding rate, and signal bandwidth, the total transmission time τ of a LoRa packet is provided by:

$$\tau = \left(20.25 + \max\left(\left\lceil \frac{(4 \cdot \text{PL} - \text{SF} + 11)}{\text{SF}} \right\rceil (\text{CR}_i + 4), 0 \right) \right) \cdot T_s, \quad (3)$$

where $\lceil \cdot \rceil$ refers to the ceil function, which gives the least integer greater than or equal to its argument. Based on the definitions above, we have that the transmission time of a LoRa packet, also defined as time-on-ir (ToA), depends on the SF and the packet size (PL) for fixed values of BW and CR_i.

Table 1. The sensitivity threshold (in dBm) for specific SF [Semtech 2017].

SF7	SF8	SF9	SF10	SF11	SF12
-124	-127	-130	-133	-135	-137

A SIR value is calculated at the receiver on the point of view of the desired signal, therefore taking into account every other interfering signals in the same logical channel. This approach does not consider non-LoRa interfering or LoRa interfering from another logical channel[3]. Then, this SIR value is compared to a threshold reported in [Goursaud and Gorce 2015] as presented in Table 2. In this table, the SIR threshold values are given in dB, each for a pair of SFs, where the row refers to desired signal's SF, whereas the column refers to the interfering signal's SF.

If the actual SIR value in any instant is above the tabulated threshold of Table 2, we consider that the packet is successfully received and forwarded to MAC layer. MAC layer creates a series of objects to keep track of available transmission time and limit transmission since LoRaWAN operates in an unlicensed band, so it is subject to duty cycle restrictions. In [Alliance 2018b], regional parameters are specified, listing the unlicensed ISM bands for the different regions worldwide.

2.2. LoRaWAN Networks

LoRa system architecture is used by LoRaWAN networks to support two important requirements as battery lifetime and long-range connectivity. A LoRaWAN network consists of one or more LoRaWAN gateways that are all connected to one central network coordinator, or so called Network Server (NS).

LoRaWAN gateways are basic protocol bridges. Each gateway receives LoRa modulated radio messages from all LoRaWAN end-devices. Every received LoRaWAN frame with a correct CRC code will be forwarded to the NS encapsulated in an IP frame. To prolong the battery life of end-devices, we should increase the number of gateways in the area, reducing the distance between them.

The LoRaWAN defines end-devices like class A, class B or class C. Class A supports bi-directional communication, the uplink message being mandatory, where the device can send an uplink message at any time and in the sequence opens two reception windows, used by NS to confirm message, at specified times of 1 s and 2 s, respectively. Class B differs from class A by adding scheduling of the receive window for downlink message from the network server, and class C differs from class A by keeping the receive window open unless they are transmitting.

---

[3]Readers interested in this topic are encouraged to obtain more information at [Semtech 2017]

Table 2. Thresholds of SIR (in dB) for all combination pairs of spreading factors [Goursaud and Gorce 2015].

desired signal	interfering signal					
	SF7	SF8	SF9	SF10	SF11	SF12
SF7	6	−16	−18	−19	−19	−20
SF8	−24	6	−20	−22	−22	−22
SF9	−27	−27	6	−23	−25	−25
SF10	−30	−30	−30	6	−26	−28
SF11	−33	−33	−33	−33	6	−29
SF12	−36	−36	−36	−36	−36	6

3. System model

The proposed analyses of LoRa are focused on the uplink communication so that the end-devices transmit messages to the gateways. The system simulations regard the EU863-870 ISM band [Alliance 2018b]. For all approaches, the channel long-distance propagation model with path-loss exponent $\alpha = 3.76$ (for the shadowed urban scenario); geographical positions of nodes are taken as a snapshot and modeled with a uniform distribution on a coverage area defined by a disk $r_{max} = 6\,000\,m$ (we carried out this study considering a small-scenario like an indoor industrial plant, and thus, all SFs are feasible options to send data from the transmitter nodes to the gateway); bandwidth $\mathrm{BW} = 125\,\mathrm{kHz}$; eight channels are available (equally spaced between 867.1 MHz and 868.5 MHz); 1% duty cycle; and coding rate CR = 1.

The multiple radio channels established throughout the cell follow models composed mainly of path-loss and obstacles, which affect the propagation profile. Buildings are uniformly created and regularly placed along a two-dimensional grid comprising the coverage area.. The positions of the gateways in such a grid are predetermined. All end-devices are class *A* devices (refer to [Alliance 2015]), and their positions are randomly sorted from a uniform distribution along the cell area and kept abiding during the simulation running time.

The instant of the first transmission of each end node is decided by a random delay via a uniform random variable in the interval from 0 and 600 seconds. After that, each end-devices randomly generates a new 28-byte packet periodically every 600 seconds.

This way, a single simulation campaign runs a plethora of transmissions from many end-devices spread over the coverage area. The thermal noise is not our primary concern, but the interference created among the end-devices sent to the same gateway is. Henceforth, we assume our scenario is interference-limited.

Then, we compute the signal-to-interference ratio (SIR) at the receiver for each message transmitted, and we consider the transmission successfully received if the SIR is above a given threshold. The thresholds we adopted were taken from [Goursaud and Gorce 2015], as summarized in Table 2.

We analyze performance exclusively in the scope of transmitting from the end-devices to the gateways. Any interactions from the gateway towards the network server are assumed to be ideal without any interfering source or bottleneck. Our simulation scenarios comprise one gateway in a single cell loaded by hundreds of end-devices.

The spreading factor for each end node is chosen and allocated as the lowest one, providing adequate receiving sensitivity (estimated based on reception power compared to Table 1) using a transmission power of 14 dBm [Alliance 2018b]. This manner of choosing the SF is the most basic SF strategy and the only one we investigate here; more advanced SF strategies can be found in [Santos F. et al. 2020]. Note that as far as the end-device is from the gateway, a higher SF is required.

Further techniques can also be adopted to enhance the reliability of the transmissions, such as a retransmission strategy. In the context of hybrid automatic repeat request (HARQ), the power of forward error correction (FEC) is combined with automatic repeat requests. If, even with FEC, the message is not satisfactorily received, relying on Table 2,

the last transmission will be repeated. Otherwise, an ACK (Acknowledgement) signal is fed back to the respective end-device transmitter, stopping the retransmission procedure.

By having two replicas of messages from the same transmitted message, we hope the receiver has more conditions to recover the right message. If, even so, the message is not correctly recovered, a new retransmission will occur. This procedure can be repeated as much as necessary until an ACK is sent to the respective end-device. Furthermore, typically, a maximal number of attempts is established.

Therefore, we expect that the reliability of the transmission is undoubtedly improved. Conversely, as the retransmission technology is enabled, the traffic offered in the network is increased, the feedback signaling is over-demanded, and more energy is drained from the transmitters' batteries. A simulation tool is an appropriate approach to quantify those benefits and drawbacks, especially for variants of HARQ.

The most straightforward retransmission technology independently deals with each replica, as described in the LoRa Alliance specifications [Alliance 2018a]. While the transmission is unsatisfactorily in accordance with Table 2 , a new retransmission shall occur. As soon as we get a satisfactory (re)transmission, just this (re)transmission is taken to Table 2, and an ACK will be sent. If, even with FEC, the message is not satisfactorily received, relying on Table 2, which does mean that a new attempt is necessary.

Even though HARQ admits some other variants, such as chase combining and incremental redundancy, we opted to explore just the former. The reason for this is that the computational and signaling complexities (aggregated to both transmitter and receiver) are much more modest with chase combining; aside from that, the performance superiority of incremental redundancy is only valid for some kinds of channels and scenarios. In [Cheng 2006], Cheng addressed the performance of chase combining and variants of incremental redundancy in-depth, albeit in a wideband code-division multiple-access (WCDMA) context. Cheng derived an analytical model and compared it with extensive simulation results. In fact, there are even more sophisticated variants of incremental redundancy, but they are out of our spotlight here since computational resources are scarce in an IoT environment.

In its optimal implementation, the chase combining does a maximum-ratio combining (MRC). In short, all received replicas are summed with different weights; each weight is the complex conjugate of the channel coefficient for the respective replica. Please note that this method depends on good channel and interference estimates to give more weight to replicas received over better SIR values; besides, it requires memory for preserving all the received versions. By extrapolating the results of [Cheng 2006] to our scenario, we look to Table 2 comparing the accumulated SIR at each retransmission simulated, which comprises the linear unweighted sum of the current retransmission SIR with the other ones that preceded it and referred to the same original message.

4. Numerical Results and Discussions

In this section, we investigate the performance of LoRa considering the availability of retransmission technology, as previously discussed. We rely on numerical results obtained from computational simulations LoRa module[4] built on the free open-source network

---

[4]The code of LoRa module is sited at `https://github.com/heldercs/loraModule`

simulator ns-3[5]. Adopting a test bed approach is unfeasible since it would require many nodes distributed throughout a large area, and changing the transmitter features is impossible due to proprietary LoRa policies.

Our goal is to reveal the expectations for adopting chase combining retransmission mechanism. We carried out this study considering a generic but illustrative scenario, where there are no priority nor traffic distinctions concerning the offered services, as well as the formats of their messages are the same, being the retransmission technology available for all the end-devices with a maximal number of three retransmissions. We also assessed the performance of LoRaWAN with retransmission without any combination of replicas. The benchmark scenario assumes the absence of retransmission technology.

For simplicity of notation, these approaches, named as chase combing of retransmissions, no combining of retransmissions, and no retransmissions, are coded as [cc RTX], [nc RTX], and [TX], respectively. For all those cases, we consider only one gateway, and a simulation campaign corresponds to a series of events comprised in one hour of system operation. Each point of packet success rate and throughput in the graphics below is obtained from the average of five independent simulation campaigns.

The transmission time-on-air τ of packets and the corresponding SF used in this analysis are shown in Table 3. The τ values were calculated using expression 3 for the following parameter values: coding rate $\mathrm{CR} = 1$; BW signal bandwidth $= 125\,\mathrm{kHz}$; data packet size for each class of $28\,\mathrm{bytes}$.

Firstly, Figure 2 presents the packet success rates separated per SF and (re)transmission approach. All SFs from 7 to 12 are simulated, but for visualization clarity, just the SFs 7, 9, and 12 are presented here. As we increase the system load in terms of total number of nodes n, the packet success rates worsen due to the fiercer competition for spectrum resources. As we increase the spread factor, the packet success rates worsen due to the largest time-on-air and, therefor, more interference. Regarding the retransmission approaches, we see a controverse behavior depending on the spread factor. For SFs 7 and 9, the absence of retransmission yields the worst case, since no remediation techniques are applied when a packet is unsuccessful. Any of both retransmission approaches improved the packet success rate, with a particular advantage to cc RTX, which, in addition to retransmitting in the event of unsuccess, makes use of all versions received. The highest SF brings a further issue once the packet collisions and interference worsen. This degradation is evident in the graphic's green lines, where the performance of both retransmission approaches was seriously hampered.

Figure 3 shows the throughput aggregated by all end-devices allocated to the same SF separated per (re)transmission approach. Again, just the SFs 7, 9, and 12 are presented, albeit all SFs from 7 to 12 are simulated. The aggregated throughput increases as we

---

[5]The website of ns-3 simulator is sited at `https://www.nsnam.org/`

Table 3. Transmission time-on-air τ (in milliseconds) of spreading factors (SF) 7, 9 and 12 [Semtech 2017].

| SF7	SF9	SF12
66.816	226.304	1646.590
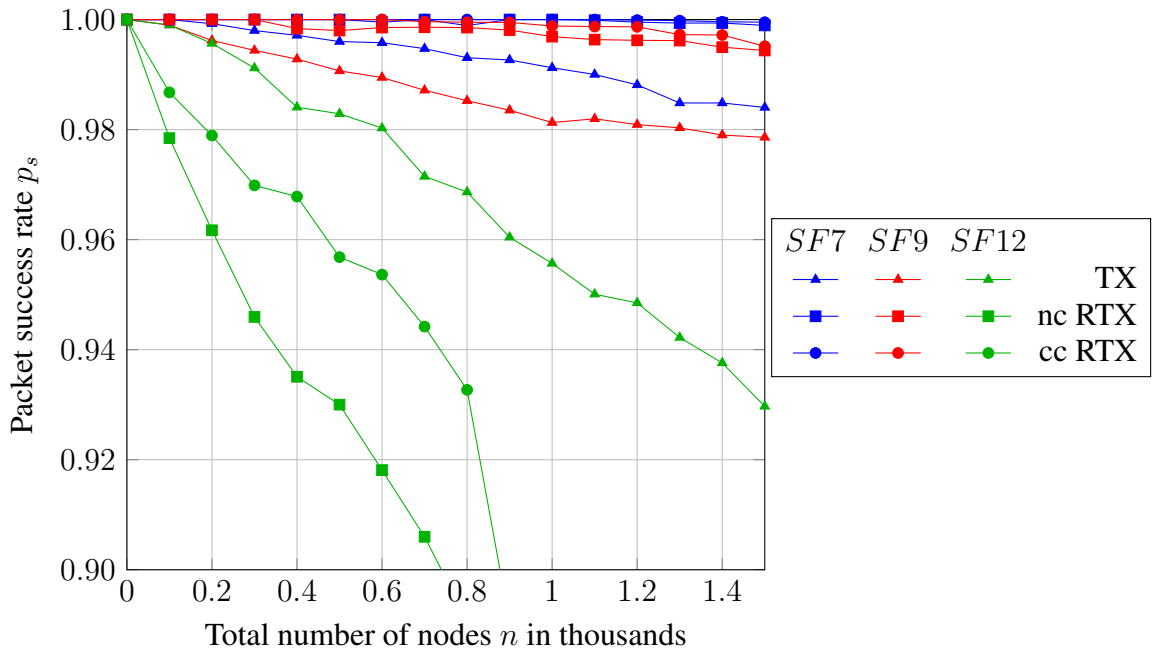
Figure 2. Packet success probability for different retransmission technologies separated for SFs 7, 9 and 12.

increase the system load. When we have high SFs, the time-on-air is extended, and the packet collisions and interference worsen, especially for high loads. This degradation is evident in the green lines of the graphic. Regarding the retransmission approaches for high spread factors, the absence of retransmission is healthier for aggregate throughput since no spectral resource will be wasted with the repetitive messages. Both nc RTX and cc RTX tried to improve each message's receiving, however, causing more interference. Aside from that, the lower the SF, the more symbols are carried and, thus, the higher the throughput, especially for cc RTX. Here, we observe the benefits of using retransmission approaches for low spread factors, since the new attempt will be helpful.

On the one hand, the retransmission approach benefits the lowest SFs; on the other, it harms the highest SFs. We end up being subject to a selective application. However, what would the general impact on the system be without entering this new field? This answer depends on the end-device's geographical distribution and SF allocation. For the sake of simplicity, we could use the well-known pathloss-based scheme [Santos F. et al. 2022], in which the whole coverage is split into complementary co-centered annuli by the pathloss without intersection between their areas.

The innermost annulus allocates SF 7 with its lighter robustness, the next outer annulus SF 8, and so on, until the outermost annulus allocates SF12, given its greater distance from the receiving antenna. If the end-devices are approximately uniformly distributed across the cell coverage, we have many more end-devices with SF12 than with SF7. All in all, the packet success rate is much better when in the absence of retransmission mechanisms, as evidenced in Figure 4, corroborating that retransmissions schemes applied in a non-selective manner are uninteresting from a systemic point of view. Still, cc RTX showed promising results, overcoming those of nc RTX. At a load of 1 000 nodes,
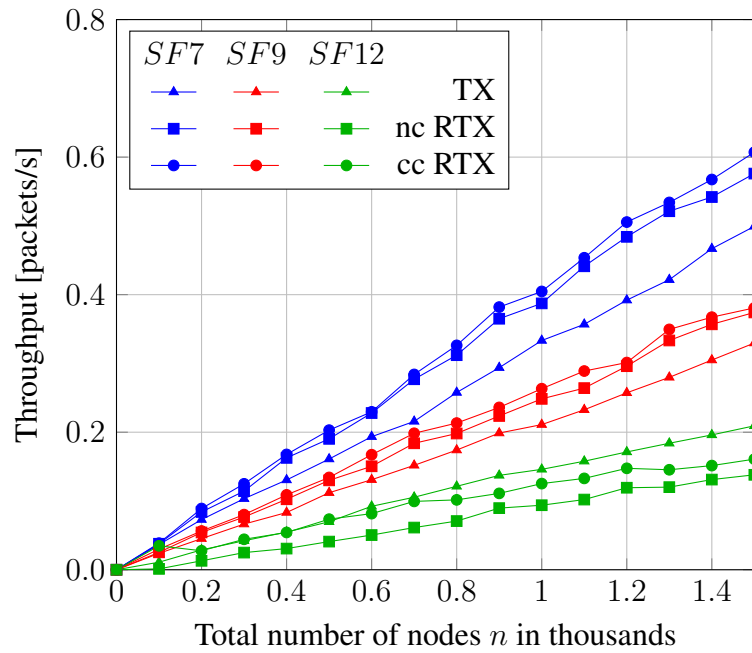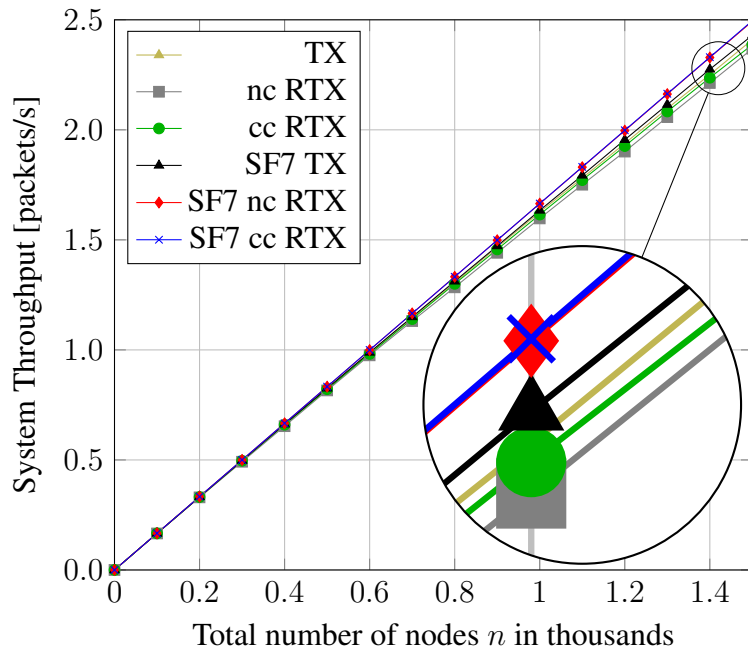
Figure 3. Throughput for end-devices for different retransmission technologies separated for SFs 7, 9 and 12.

for instance, the packet success rate was 0.97566 for TX, 0.96892 for cc RTX, and 0.95849 for nc RTX. Similar conclusions can be drawn from Figure 5, albeit on a smaller scale.
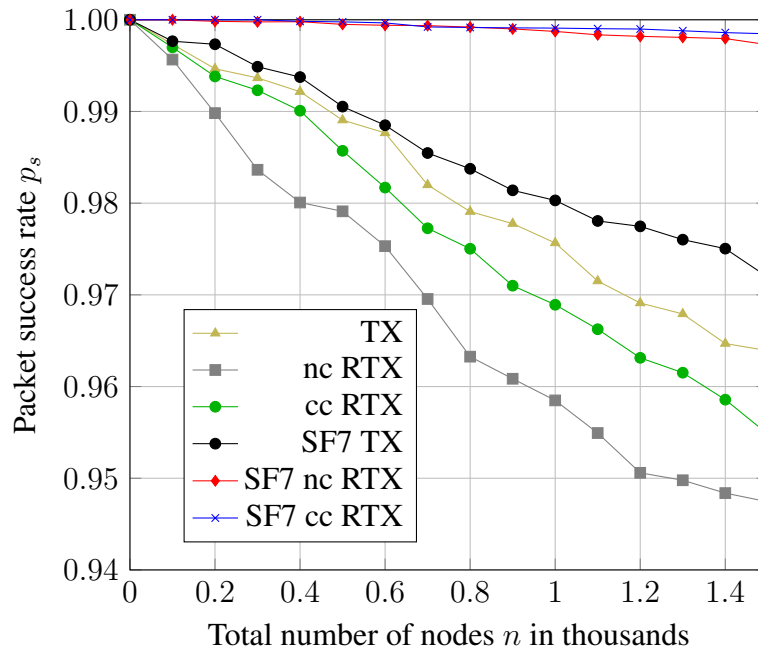
Figure 4. System packet success probability for devices for different retransmission technologies. Three curves represent the performance for the usual system comprising the SFs from 7 to 12; other three curves represent the performance with all end-devices allocated solely to the SF 7.

The higher SFs are harmful not only for themselves. The long time-on-air combined with retransmissions becomes a strong interference for the system as a whole. As we already know, the orthogonality between different SFs is imperfect [Croce et al. 2018]. It depends on the spread factors and the receiving powers involved. Moreover, orthogonality is even more harmed by fading in the channel. Hence, we created a test scenario in which all the end-devices are allocated solely to the SF7. This way, we drastically reduce the harshness of the source of interference, as illustrated in the above-mentioned Figures 4 and 5. Now, the performance of retransmission impressively overcomes TX, which corroborates that the retransmissions did not bring severe side effects in that test scenario. For the load of $1\,000$ nodes, for instance, while TX presented a packet success rate of 0.98030, nc RTX reaches 0.99873 and cc RTX 0.99909.

Figure 5. System throughput for different retransmission technologies. Three curves represent the performance for the usual system comprising the SFs from 7 to 12; other three curves represent the performance with all end-devices allocated solely to the SF 7.

In order to probe how exactly LoRA demands the retransmission, we should examine how many times some retransmission was unnecessary, how many times one retransmission was necessary and enough, how many times two or three retransmissions were required, and so on. As previously explained, the retransmission procedure in LoRa operates in a periodic loop that terminates when an ACK is received or when it reaches the maximum number of attempts. The last retransmission before a stop is indexed as 0, 1, 2, or 3. These numbers refer to the original transmission and subsequent retransmissions.

Figure 6 shows the distribution of the last retransmission index for the highest low load, say 1500 end-devices, except for index 0. For simplicity of graphic visualization, we omitted the index 0 occurrences and SFs 8, 10 and 11. Note that the total number (i.e., aggregating SFs 7, 9, and 12) of occurrences of retransmission in each technology is approximately the same, 356 on average, once there is no difference in the reliability

regarding the original transmission. Nonetheless, there is an expressive difference between nc RTX and cc RTX regarding how this total number of retransmissions is split into different indexes of the last retransmission.

The sum of occurrences of the index from 1 to 3 of nc RTX approximates the number of unsuccessful packets of the TX approach. In contrast, the total number of occurrences at index 0 of nc RTX or cc RTX are almost the same number of successful packets of the TX. Both nc RTX and cc RTX allow a new attempt for a failed transmission, while the TX approach promptly gives up.

Noticeably, cc RTX has a more significant number of stops at the first retransmission index than in nc RTX, implying that cc RTX can deliver a successful packet with fewer retransmissions than nc RTX. Thereby, the delay experienced and drained energy is reduced in favor of cc RTX.

Undoubtedly, any retransmission implies an additional delay in the message. Since the retransmission will occur in the absence of ACK into two receiving windows, we can assume that this additional delay is t_r. For the sake of simplicity, let us assume t_r is a constant value. If the first index of retransmission is required, the delay will be t_r in addition to the time already spent transmitting the original message (index 0 of retransmission). If the second index of retransmission is required, two other attempts were made before, representing an additional delay of $2t_r$. If the third index of retransmission is required, it means that three other attempts were made before, representing an additional delay of $3t_r$. Thus, by doing a weighted sum of the number of retransmissions, we obtain a surplus delay of $575\, t_r$ to nc RTX and of $540\, t_r$ to cc RTX about TX.

Similarly, we can analyze it in terms of transmission energy. The system spent P_r in power, thus draining energy from devices' batteries for each transmission or retransmission given by $P_r T$, where T is the duration time of transmission. Saving the energy of aggregated transmitters means expanding the lifespan of the many battery-operated sen-
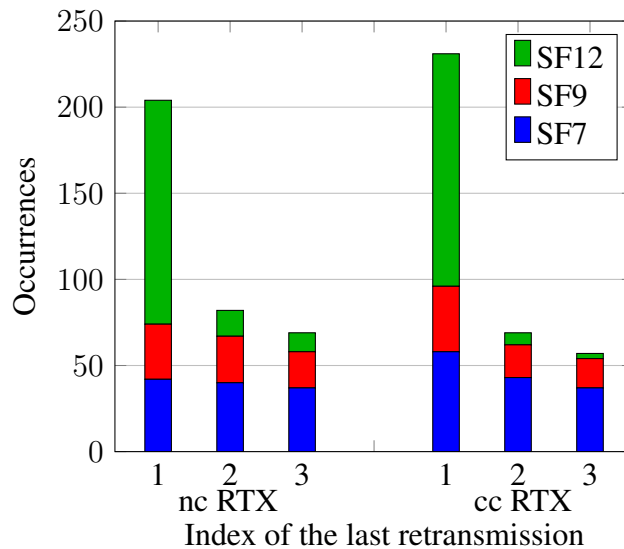
Figure 6. Number of retransmission occurrences for $n = 1500$ **end-devices for different retransmission technologies. Just SF7, SF9 and SF12 are presented.**

sors. Basically, we save energy if we do not retransmit, requiring just P_rT to be drained from the aggregate of devices' batteries. Otherwise, in the case, we stopped after the first retransmission, $2P_rT$ is drained; in the case we stopped after the second retransmission, $3\ P_rT$ is drained; and finally, in the case we stopped after the third retransmission, $4\ P_rT$ was drained. Therefore, the weighted sum here yields to $4686\ P_rT$ of consumption for nc RTX and $4682\ P_rT$ for cc RTX, contrasting to $4322\ P_rT$ for TX.

Regarding the allocation of SF, it is important to note that lower SFs may be more susceptible to interference. However, they are typically assigned to end-devices in close proximity to the gateway in order to offset their slightly reduced robustness. As a result, all SFs are subject to similar transmission failure rates.

5. Conclusions

This investigation has illuminated the attractiveness of chase combining-based retransmissions in LoRaWAN. Our studies, grounded in numerical results, underscore the multifaceted significance of HARQ in addressing the challenges associated with prioritizing critical services. Incorporating chase combining in LoRaWAN proves pivotal for enhancing the reliability of transmitting uplink packets. The benefits of retransmission technology are best utilized when the interference is not too severe, which is closely related to time-on-air. Therefore, the benefits of retransmission are awe-inspiring, especially for low spread factors, as we discovered through extensive simulation campaigns. The delay and energy consumption are unavoidable side effects of any retransmission technology. Our analysis has revealed that chase combining reduces these side effects compared to standard retransmission technology, aligning with the imperative to extend the lifespan of battery-operated sensors.

The deployment of chase combining retransmission in LoRaWAN is more than merely a technological enhancement to be addressed for forthcoming specification. Rather, it is a crucial element that ensures reliability at modest energy expenses and delays in the realm of LoRAWAN technologies. Moving forward, the findings presented herein catalyze further exploration of selective or opportunistic adoption of chase combining technology. This will contribute to the ongoing evolution of resilient and efficient communication frameworks in the era of IoT.

References

Abdelfadeel, K. Q., Zorbas, D., Cionca, V., and Pesch, D. (2020). $free$ —fine-grained scheduling for reliable and energy-efficient data collection in lorawan. *IEEE Internet of Things Journal*, 7(1):669–683.

Adelantado, F., Vilajosana, X., Tuset-Peiro, P., Martinez, B., Melia-Segui, J., and Watteyne, T. (2017). Understanding the Limits of LoRaWAN. *IEEE Communications Magazine*, 55(9):34–40.

Ahmed, A., Al-Dweik, A., Iraqi, Y., Mukhtar, H., Naeem, M., and Hossain, E. (2021). Hybrid automatic repeat request (harq) in wireless communications systems and standards: A contemporary survey. *IEEE Communications Surveys & Tutorials*, 23(4):2711–2752.

Alliance, L. (2015). LoRaWAN, what is it?. a technical overview of lora and LoRaWAN. *White Paper*.

Alliance, L. (2018a). LoRaWAN specifications v1.0.3. *LoRa Alliance: Fremont, USA*.

Alliance, L. (2018b). LoRaWANtm 1.1 regional parameters. *LoRa Alliance*.

Capuzzo, M., Magrin, D., and Zanella, A. (2018). Confirmed traffic in lorawan: Pitfalls and countermeasures. *17th Annual Mediterranean Ad Hoc Networking Workshop (Med-Hoc-Net 2018)*, pages 87–93.

Cheng, J.-F. T. (2006). Coding Performance of Hybrid ARQ Schemes. *IEEE Transactions on Communications*, 54(6):1017–1029.

Croce, D., Gucciardo, M., Mangione, S., Santaromita, G., and Tinnirello, I. (2018). Impact of lora imperfect orthogonality: Analysis of link-level performance. *IEEE Communications Letters*, 22(4):796–799.

de Castro Tomé, M., Nardelli, P. H., and Alves, H. (2018). Long-range Low-power Wireless Networks and Sampling Strategies in Electricity Metering. *IEEE Transactions on Industrial Electronics*, 66(2):1629–1637.

Goursaud, C. and Gorce, J.-M. (2015). Dedicated networks for iot: Phy/mac state of the art and challenges. *EAI endorsed transactions on Internet of Things*.

Haxhibeqiri, J., De Poorter, E., Moerman, I., and Hoebeke, J. (2018). A survey of LoRaWAN for iot: from technology to application. *Sensors*, 18(11):3995.

Lee, J., Yoon, Y. S., Oh, H. W., and Park, K. R. (2021). Dg-lora: Deterministic group acknowledgment transmissions in lora networks for industrial iot applications. *Sensors*, 21(4).

Mahmood, A., Sisinni, E., Guntupalli, L., Rondón, R., Hassan, S. A., and Gidlund, M. (2018). Scalability analysis of a lora network under imperfect orthogonality. *IEEE Transactions on Industrial Informatics*, 15(3):1425–1436.

Paul, B. (2020). A novel mathematical model to evaluate the impact of packet retransmissions in lorawan. *IEEE Sensors Letters*, 4(5):1–4.

Santos F., F. H. C., Dester, P. S., Nardelli, P. H. J., Stancanelli, E. M. G., Cardieri, P., Carrillo, D., and Alves, H. (2022). Multi-class random access wireless network: General results and performance analysis of LoRaWAN. *Ad Hoc Networks*, 135:102946.

Santos F., F. H. C., Dester, P. S., Stancanelli, E. M. G., Cardieri, P., Nardelli, P. H. J., Carrillo, D., and Alves, H. (2020). Performance of LoRaWAN for handling telemetry and alarm messages in industrial applications. *Sensors*, 20(11).

Semtech (2017). *SX1272/73 860 MHz to 1020 MHz Low Power Long Range Transceiver*. Semtech Corporation. Rev. 3.1.

Vangelista, L. (2017). Frequency shift chirp modulation: The LoRa modulation. *IEEE Signal Processing Letters*, 24(12):1818–1821.